The British Journal of Radiology, 84 (2011), S112–S120

Dynamic contrast-enhanced imaging techniques: CT and MRI

[1]J P B O'CONNOR, FRCR, PhD, [2]P S TOFTS, PhD, [2]K A MILES, FRCR, MD, [1]L M PARKES, PhD, [1]G THOMPSON, MRCS and [1]A JACKSON, FRCR, PhD

[1]*Imaging Science, Proteomics and Genomics Research Group, University of Manchester, Manchester, UK, and* [2]*Brighton and Sussex Medical School, Falmer, UK*

ABSTRACT. Over the last few decades there has been considerable research into quantifying the cerebral microvasculature with imaging, for use in studies of the human brain and various pathologies including cerebral tumours. This review highlights key issues in dynamic contrast-enhanced CT, dynamic contrast-enhanced MRI and arterial spin labelling, the various applications of which are considered elsewhere in this special issue of the *British Journal of Radiology*.

DOI: 10.1259/bjr/55166688

The tumour microvasculature can readily be imaged using X-ray, CT and MRI techniques. This review concentrates on three main methods. Dynamic contrast-enhanced CT (DCE-CT) and dynamic contrast-enhanced MRI (DCE-MRI) are well-established techniques, where data acquisition and analysis are comparable despite inherent differences in signal production and mechanism of tissue contrast enhancement (reviewed in [1, 2]). Although they can be performed on conventional clinical scanners, they require specialist image analysis to extract biomarkers of tumour vascular function. In distinction, arterial spin labelling (ASL) offers a highly specific method of measuring cerebral perfusion without exogenous contrast agent (CA) administration, but is at present a research technique. The practical applications of these techniques are considered elsewhere in this special issue.

Basic principles of dynamic contrast-enhanced imaging

DCE imaging describes the acquisition of a baseline image(s) without contrast enhancement followed by a series of images acquired over time after an intravenous bolus of conventional CA. The presence of CA within cerebral blood vessels and tissues affects measured X-ray attenuation on CT in a linear fashion and the calculated signal intensity on MRI in a non-linear manner. Thus, the temporal changes in contrast enhancement effectively provide a time–concentration curve, which can be analysed to quantify a range of physiological parameters that indicate the functional status of the vascular system within tumours and adjacent tissues. These parameters reflect the two-compartment pharmacokinetics exhibited by CA, comprising intravascular and extravascular components. During the first-pass of the CA through the circulation (typically 45–60 s after injection), CA is predominantly intravascular allowing evaluation of perfusion (*i.e.* blood flow per unit volume or mass of tissue), relative blood volume (rBV) and mean transit time. During the subsequent 2–10 min, there is increasing passage of CA into the extravascular space, and imaging during this delayed phase enables measurement of vascular permeability and relative extravascular volume.

Address correspondence to: Dr J P B O'Connor, Imaging Science, Proteomics and Genomics Research Group, Stopford Building, Oxford Road, University of Manchester, Manchester M13 39T, UK. E-mail: james.o'connor@manchester.ac.uk

DCE-CT image acquisition protocols

A number of distinct DCE-CT techniques have been developed, reflecting the different analysis methodologies adopted by commercial software packages for perfusion CT. The main acquisition factors to be considered are summarised in Table 1. For DCE-CT, the need to keep the radiation burden as low as practicable is a constraint on the total number of images acquired and the X-ray exposure factors. Nevertheless, the choice of protocol is primarily determined by the physiological parameters to be measured and the analysis methodology. There are essentially two approaches to analysis: compartmental modelling and deconvolution. Detailed descriptions of these approaches can be found elsewhere [3]. The dependence of acquisition parameters on analysis methodology relates to the different assumptions used in their respective models. A short sharp bolus of CA is particularly important for first-pass studies analysed with a compartmental model. Images acquired for compartmental analysis can also be successfully processed using deconvolution analysis. To date, no consensus has emerged as to which perfusion CT technique is optimal for the assessment of tumour vascularity.

Processing DCE-CT data

Semi-quantitative parameters

Semi-quantitative parameters that reflect tumour vascularity are readily obtained from tumour time–attenuation curves obtained during DCE-CT (Table 2).

Table 1. Summary of image acquisition parameters for dynamic contrast-enhanced CT

Overall length of time of the image series	First pass imaging for perfusion and rBV Delayed imaging for vascular permeability
The number and frequency of images	First pass: no slower than one image every 2–3 s Delayed phase: one image every 5–10 s
The number and thickness of CT slices	Constrained by the width of the CT detector Detector can be divided into several slices (*e.g.* 4 × 5 mm) ''Table-toggling'' allows greater volumes
X-ray exposure factors	Lower tube voltages (*i.e.* 80–100 kVp) reduce radiation dose and increase in X-ray attenuation of contrast material Lower tube current and higher image frequency Suitable for deconvolution analysis Compartmental modelling favours higher tube current (with reduce image frequency to minimise radiation dose)
Type of contrast medium	Non-ionic contrast medium preferred Different agents may produce different values for vascular permeability
Volume and concentration of contrast medium	Volume 40–50 ml Rapid injection rate ($\geq$4 ml s^{-1}; 7 ml s^{-1} for compartmental models) and high iodine concentration (*i.e.* 350–400 mg) to maximise contrast enhancement Biphasic injections may be useful for vascular permeability measurements derived from compartmental modelling

rBV, relative blood volume.

Clinicopathological studies have shown that many of these parameters correlate with the density of microvessels within a range of tumours [4–6]. This correlation suggests that, although simple in derivation, some of these parameters are related to perfusion normalised to cardiac output. This normalisation is an advantage because it inherently corrects for individual variations in cardiovascular function that might otherwise alter tumour perfusion despite no change in microvessel density. However, when using semi-quantitative parameters, it is also important to calibrate the CT system because significant variations in iodine sensitivity can exist between CT systems or on the same CT system over time [7].

Absolute quantification

In addition to data from the tissue itself, derivation of discrete physiological parameters also requires a time–attenuation curve from a supplying artery, known as the arterial input function (AIF). Within the brain, these arteries are small and therefore time–attenuation data from the sagittal sinus is used to correct for partial volume effects. The parameters commonly obtained from DCE-CT are summarised in Table 3. For capillary beds that are highly permeable, measurements of vascular leakage will approximate perfusion.

DCE-CT measurements of perfusion and blood volume in cerebral tissues and brain tumours have been validated against a range of reference methods, including microspheres in animals and xenon-CT in humans. Reproducibility has been shown to be good for absolute quantification of DCE-CT with typical test–retest values for perfusion in normal brain and tumour of 7–13% [8, 9]. Table 4 shows a set of three illustrative acquisition and analysis procedures, typical of those in current use. Table 5 shows the accepted standardised abbreviations for microvascular parameters derived from dynamic MRI.

Image segmentation

Software packages for analysis of DCE-CT data typically include automated or semi-automated processes to identify particular structures to improve the accuracy and reproducibility of results. Brain tissue is readily separated from non-cerebral tissues using attenuation thresholds on baseline images while the arterial input and sagittal sinus can be segmented from contrast-enhanced images. Algorithms that use enhancement thresholds or perfusion values to remove large vessels within tumour regions can also improve the accuracy of perfusion measurements but should be used with care for highly vascular tumours such as meningiomas. It is also possible to automatically segment cerebral grey and white matter as well as enhancing and non-enhancing regions of tumour [10].

Table 2. Semi-quantitative parameters from dynamic contrast-enhanced CT

Peak enhancement	Affected by dose of contrast material, patient weight and iodine calibration factor
Perfusion normalised to cardiac output	Peak enhancement corrected for dose of contrast material and iodine calibration factor
Standardised perfusion value	Peak enhancement corrected for iodine calibration factor and patient weight
Area under the time–attenuation curve	Related to blood volume but affected by dose of contrast material and iodine calibration factor
Maximum upslope	Related to perfusion but affected by peak arterial enhancement

Table 3. Common parameters that can be absolutely quantified by dynamic contrast-enhanced CT

Parameter	Units
Perfusion	ml min^{-1} ml^{-1} or ml min^{-1} 100 g^{-1} tissue
Relative blood volume	ml ml^{-1}, ml 100 g^{-1} or %
Mean transit time	s
Permeability–surface area product	ml min^{-1} ml^{-1} or ml min^{-1} 100 g^{-1} tissue
Relative extravascular volume	ml ml^{-1}, ml 100 g^{-1} or %

Advantages and disadvantages of DCE-CT

The need to use ionising radiation is an important limitation for DCE-CT. However, with typical radiation doses of 1–2 mSv, the radiation burden is similar to xenon-CT and O-15 positron emission tomography (PET) but less than single photon emission tomography. The restricted anatomical coverage in the cranial-caudal direction is a further constraint for DCE-CT but less so as larger detector tracks and table-toggling techniques become available [11]. The increasing availability of 256 slice scanners also makes whole brain DCE-CT at an acceptable radiation dose available at many centres. The CT CAs are more viscous, and bolus duration is often longer than in MRI.

The main advantage of DCE-CT is its simplicity in terms of acquisition and processing. The linear relationship between CA concentration and X-ray attenuation aids absolute quantification with commercial software approved by the United States Food and Drugs Administration available from most CT manufacturers. DCE-CT also benefits from wide availability and low cost. The high spatial resolution of CT supports accurate placement of regions of interest and results in high-resolution parametric images. For the brain, the reproducibility of DCE-CT measurements approaches that of PET and may be superior to DCE-MRI [12].

Opportunities for application of DCE-CT

DCE-CT can be readily incorporated into existing CT protocols, including CT angiography. DCE-CT can also be performed using integrated PET/CT systems, enabling tumour vascularity and glucose metabolism to be evaluated simultaneously. This combined information offers new insights into tumour pathophysiology with the potential to assess tumour aggression [13].

Basic principles of DCE-MRI

DCE-MRI uses the same principles as DCE-CT. A dynamic image acquisition is performed during which an intravenous bolus of standard small molecular weight gadolinium-based CA is injected intravenously. Images of the resultant changes in signal intensity can then be analysed to derive parametric maps of specific micro-vascular biomarkers. There are a number of significant differences between CT and MR-based approaches. One of the major factors is that changes in MR signal are not linearly related to changes in CA concentration. MR images can be acquired using either T_2* or T_2 weighting (T_2 weighted DCE-MRI, also known as dynamic susceptibility contrast MRI or DSC-MRI) or T_1 weighting (T_1 weighted DCE-MRI). These different contrast mechanisms have a major impact on the nature of the signal changes observed and the analytical approaches applied to the data.

Dynamic susceptibility contrast MRI

In DSC-MRI, rapid loss of MR signal on T_2 or T_2* weighted images is measured and then used to calculate the change in concentration of CA for each individual voxel (Figures 1 and 2). A series of pre-contrast images are acquired for approximately 1 min to enable an estimate of baseline CA concentration to be made. Gadolinium CA is then administered through an automated injection pump as an intravenous bolus (to achieve a relatively uniform rate and volume of injected CA), followed by a saline flush and a series of acquisitions are made over a few minutes. The signal intensity–time course data acquired for each image can then be transformed into a measure of CA concentration by calculating the change in the effective transverse relaxation rate (R_2*),

Table 4. Acquisition and processing parameters for three illustrative perfusion CT protocols for the assessment of tumour vascularity

	1	2	3
Contrast medium			
Concentration	370 mg ml^{-1}	370 mg ml^{-1}	370 mg ml^{-1}
Volume	40 ml	50 ml	100 ml
Injection rate	4–7 ml s^{-1}	7–10 ml s^{-1}	4 ml s^{-1}
Acquisition type	Single location	Single location	Multiple spiral
Slice thickness	4 × 5 mm	2 × 10 mm	20 × 3 mm
No. of images	60	15	6
Image frequency	Every 1 s	Every 3 s	Every 20 s
Tube current	50–100 mAs	100–250 mAs	100–250 mAs
Analysis method	Deconvolution for perfusion and blood volume	Compartmental analysis for perfusion and blood volume	Standardised perfusion value Patlak analysis for permeability and blood volume
Advantages	Good temporal resolution High spatial resolution	Low image noise	Large volume coverage High spatial resolution
Disadvantages	Image noise Limited volume coverage	Reduced temporal resolution Limited volume coverage	Poor temporal resolution

Table 5. Common parameters derived from advanced MRI methods that evaluate the tumour microvasculature

Symbol	Short name	Unit
Estimated or predetermined quantities		
MTT	Mean transit time	s
CTT	Capillary transit time	s
Calculated parameters		
F	Perfusion (blood flow per unit volume of tissue)	$ml\,min^{-1}\,ml^{-1}$
CBF	Cerebral blood flow per unit volume	$ml\,min^{-1}\,ml^{-1}$
P	Total capillary wall permeability	$cm\,min^{-1}$
PS	Permeability–surface area product per unit mass of tissue	$ml\,min^{-1}\,g^{-1}$
E	Extraction fraction	None
K^{trans}	Volume transfer constant between plasma and EES	min^{-1}
CBV	Cerebral blood volume per unit of tissue	ml^{-1}
v_p	Fractional blood plasma volume	%
v_e	Volume of EES per unit volume tissue	%
IAUC	Initial area under gadolinium concentration agent–time curve	mM min

EES, extracellular extravascular space.

$$\Delta R_2* = \frac{-\ln(S(t)/S(0))}{\mathrm{TE}} \quad (1)$$

where $S(0)$ is the baseline signal intensity, $S(t)$ is the pixel intensity at time t and TE is the echo time.

Fast imaging techniques are used to enable rapid measurements of signal change, since proper characterisation of the bolus (and subsequent T_2 or T_2* weighted signal loss) requires sampling of the signal with a high temporal resolution (typically a few seconds or less), while keeping a long enough TE. Both single or multi-shot echo planar imaging (EPI) and fast low angle shot (FLASH) can achieve this temporal resolution, but vary in the number of slices that may be acquired: EPI sequences can typically acquire up to 15 slices (matrix resolution 128×128 or greater) within this time frame [14, 15]. Three-dimensional volumetric sequences have been employed in an attempt to increase volume coverage at the expense of either spatial or temporal resolution [16].

The susceptibility contrast mechanism results from changes in local field strength within the tissue induced by the paramagnetic contrast molecules [17]. These variations affect water molecules at some distance from the contrast so the apparent CA concentration measurements will be affected by the local vascular structure. A given amount of contrast in a diffuse capillary bed will have a larger effect than the same amount of contrast concentrated in a single large vessel, since the local changes in field strength will be more widely dispersed. This has led to widespread use of DSC-MRI to study changes in grey and white matter, since the signal-to-noise ratio (SNR) is consequently far better than can be achieved with T_1 weighted techniques in the presence of low tissue CBV. Similarly, imaging of signal changes resulting from T_2* and matched T_2 weighted sequences, where susceptibility effects are far smaller, allow extraction of information concerning the size and distribution of blood vessels within the voxel, so-called ''vessel size imaging'' [18].

Another major feature of susceptibility-based images is that T_1 effects commonly contaminate them. Thus, a signal loss due to the T_2* effect of intravascular contrast will be countered by a signal gain due to the T_1 effects of contrast that has leaked into the perivascular tissue. DSC-MRI techniques for use in tumours, where vessels are commonly sufficiently permeable to allow leakage of contrast, need to be designed to minimise this ''T_1 shine-through'' in order to avoid systematic underestimation of

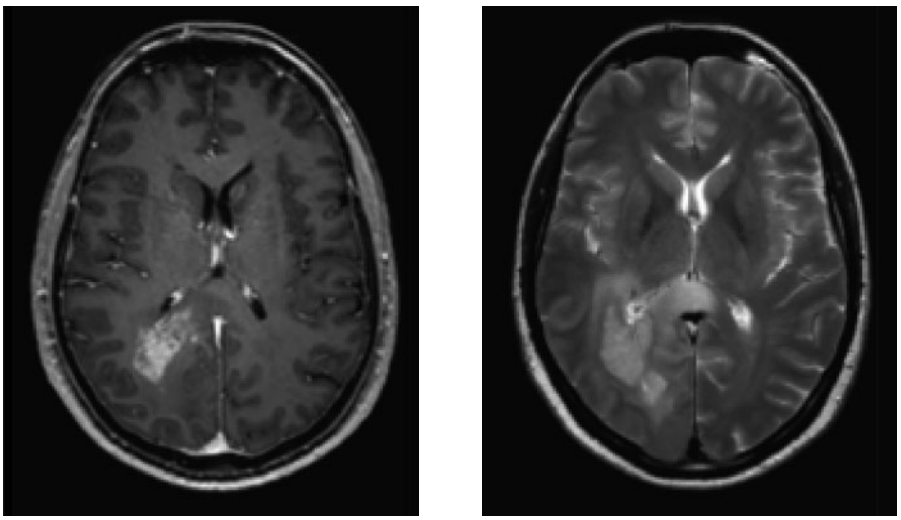

(a) (b)

Figure 1. (a) Post-contrast T_1 weighted and (b) T_2 weighted images showing an enhancing glioblastoma adjacent to the posterior horn of the right lateral ventricle.

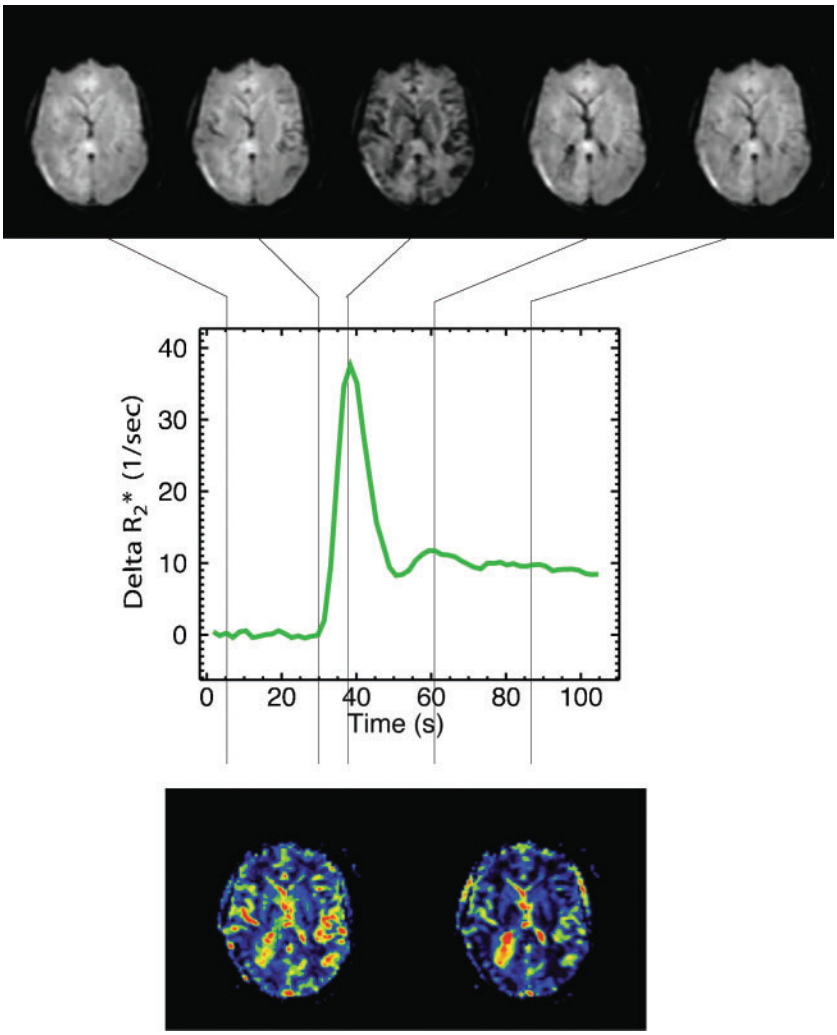

Figure 2. T_2 weighted dynamic contrast-enhanced MRI in the patient shown in Figure 1. (Top) Dynamic time course series through the brain using a T_2* weighted acquisition during passage of bolus of contrast agent. There is decrease in signal intensity within the brain as the contrast agent bolus traverses the grey and white matter. (Middle) Plot of contrast concentration changes in tumour. (Bottom) Calculated images of blood flow (right) and blood volume (left) showing increased flow and blood volume within the tumour.

CBV. This can be done by reducing the flip angle, and hence the T_1 and sensitivity, of the commonly used gradient echo sequences. However, this reduces the SNR in the remaining time course data. An alternative approach is to pre-dose the patient with a contrast injection given 5–10 min before the DSC-MRI acquisition [19]. Despite these significant problems, the ease of acquisition and analysis has meant that the DSC-MRI has become one of the most widely used dynamic enhancement techniques in brain tumour studies and clinical practice.

The analysis of the DSC-MRI data has been discussed in detail elsewhere [17]. Usually relatively simple metrics are derived, particularly regional CBV, which can be estimated from the area under the first pass component of the contrast concentration–time course curve. DSC-MRI measurements of CBV represent the most commonly used and best validated microvascular biomarkers used in cerebral tumour studies. Similar basic analytical approaches provide estimates of mean transit time (MTT) and contrast arrival time parameters (T0, and the time to peak (TTP), although these have found relatively little application in cerebral tumours. Estimation of absolute flow is complex and has been the basis of many methodological studies. In principle, the concentration–time course data from an individual tumour voxel can be deconvolved with an arterial input function, derived from a major vessel, to produce a direct measurement of flow. In practice, these measurements are complicated by variations in regional contrast arrival times and by dispersion of the contrast bolus within the vascular tree [20]. Since it is impossible to identify with any accuracy the vessel supplying a region of tumour, these methods have not been widely applied in tumour studies. In malignant tumour capillary beds, there are areas of low perfusion pressure, which are characterised by intravascular trapping of the CA. This effect, originally recognised on cerebral angiography, can also be quantified using DSC-MRI data to measure the extent to which the contrast concentration returns to normal after passage of the first bolus of contrast. This parameter, called relative recirculation (rR) has also been shown to be of significant value as a biomarker in a number of tumour studies [19].

In tissues, such as malignant tumours, where considerable leakage of contrast occurs from the vessels into the extravascular extracellular space it is theoretically possible to calculate estimates of the endothelial permeability of the capillary bed using DSC-MRI data. However, the characteristics of the signal change and the underlying problems of T_1 shine-through make such analyses relatively unreliable. Consequently, there has been an increased interest in the use of T_1 weighted DCE-MRI techniques where the application of this type of analytical approach is more reliable.

T_1 weighted DCE-MRI

Dynamic MRI can also be used to derive estimates of a number of parameters that describe the microvascular environment including direct estimates of capillary endothelial permeability (Figure 3) [17]. This is of particular interest since drugs that target the vascular endothelial growth factor (VEGF)-1 and -2 receptor cause rapid reductions in capillary permeability within the tumour. The methodology is similar to those described above: a T_1 weighted multislice or volume imaging sequence is run repeatedly, typically every few seconds. A bolus injection of the CA is given, and the subsequent image enhancement is measured for about 5 min. Protocol variations reflect trade-offs between spatial resolution (typically a few millimetres), temporal resolution (how quickly each image is acquired) and extent of anatomical coverage. Ideally a measurement of baseline T_1 before gadolinium injection is required, to enable transformation of the signal intensity-time curve into a time–concentration curve (TCC). This is used together with the known relaxivity of the CA and a model of how signal depends on T_1 for the particular sequence used to calculate contrast concentrations in each frame of the dynamic image series. The shape of the tumour signal intensity-time curve and TCC contain information about the rate of uptake and clearance of gadolinium and can be analysed to derive a number of potential biomarkers of the vascular microenvironment.

Analysis of T_1 wDCE-MRI data

Depending on the analysis approach chosen, measurements may be derived from signal intensity data, or more commonly, signal intensity data are transformed into contrast concentration data prior to analysis. Analysis may be performed on a region of interest or, less commonly, on a pixel-by-pixel basis. Simple semi-quantitative metrics can be derived from the tissue residue function alone. More complex pharmacokinetic-based analyses require identification of an AIF. The AIF may be measured in a major blood vessel, often the carotid middle cerebral artery. Derivation of the AIF is far from straightforward and is discussed in detail elsewhere [21]. In brain tumour studies, a signal intensity time curve from the sagittal sinus is commonly used as a surrogate AIF since it is relatively simple to identify and is robust to partial volume artefacts. However, where this is done a correction must be made for the delayed

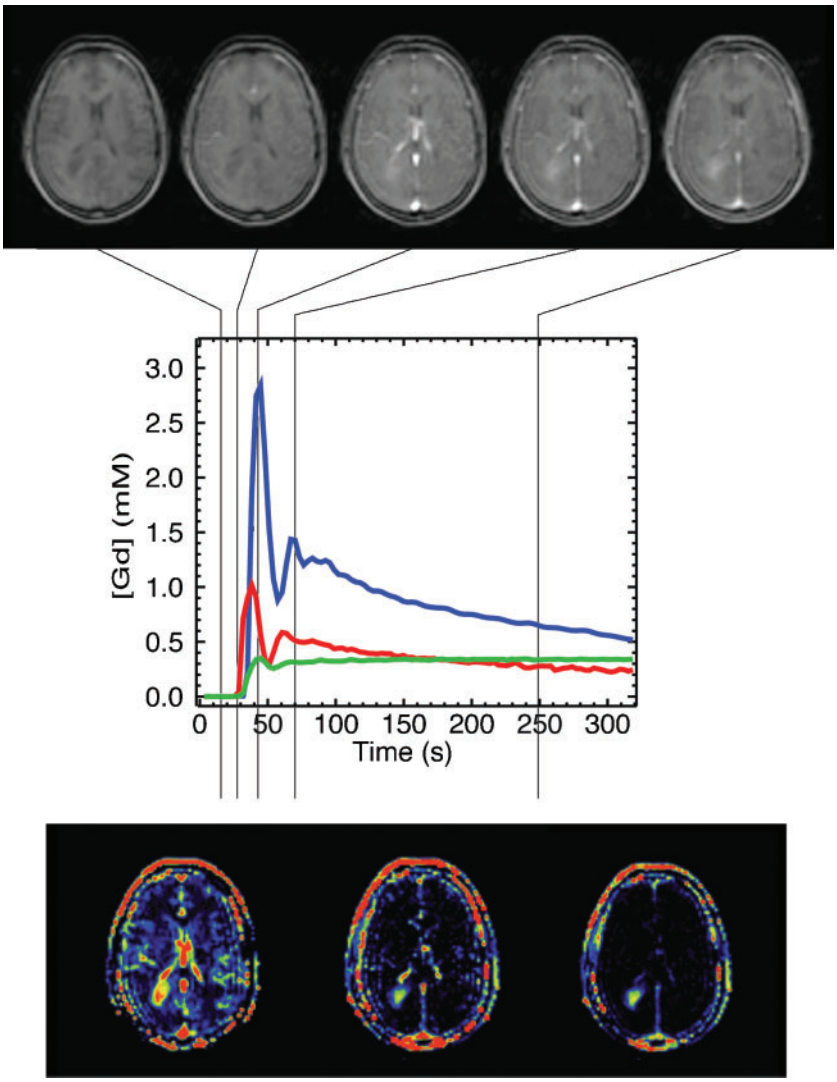

Figure 3. Dynamic T_1 weighted dynamic contrast-enhanced MRI in the patient shown in Figure 1. (Top) Dynamic time course series through the brain using a T_1 weighted acquisition during passage of bolus of contrast agent. There is increase in signal intensity within the brain as the contrast agent bolus traverses the grey and white matter. Early persistent enhancement is seen in the tumour. (Middle) Concentration–time course curves from the middle cerebral artery (red), superior sagittal sinus (blue) and tumour (green). (Bottom) Parametric maps of v_p (left), K^{trans} (centre) and v_e (right).

arrival of the CA within the venous system. Alternatively, an idealised input function or population-based function [21] may be used.

Simple features of the signal–time or contrast concentration–time curves (such as gradient or time to 90% peak enhancement) can easily be extracted without knowledge of an AIF [22]. The integrated area under the CA concentration–time curve (IAUC) is one of the most commonly used metrics, and has been shown to be robust to measurement error and highly reproducible- [23]. These simple semi-quantitative metrics have been used extensively in diagnostic practice with considerable benefit, particularly in the study of breast cancer.

In the majority of reported studies, analysis is performed using pharmacodynamic models to describe the relationship between the tumour and blood TCC. The available analytical models differ in the degree of physiological specificity that they seek to provide. The most complex models, such as the adiabatic tissue homogeneity model [24], include estimates of blood flow (F), proportional blood volume (v_p), capillary permeability surface area product (PS) and the proportional volume of the extravascular extracellular distribution space [EES (v_e)]. Although this degree of biological specificity is desirable, significant analytic problems make its application inappropriate in the majority of cases. The majority of pharmacokinetic analyses rely on curve-fitting methods to produce estimates of parametric values. The accuracy of curve-fitting techniques is affected by the temporal resolution of the data, the SNR and the number of free-fitting parameters in the function. Consequently, the accuracy of parametric estimates will be directly affected by the data quality and the choice of analytical model [25, 26]. Although acquisition sequences can be modified to optimise data quality, there is an inevitable trade-off between temporal resolution, SNR and tissue coverage. Furthermore, if analysis is to be performed on a voxel-by-voxel basis then the SNR of individual voxels will become the limiting factor. In most tumours this will be heterogeneous, and some steps may have to be included in the analysis to identify voxels where data quality is too poor to support analysis. The commonest approach to these problems is to use a simplified pharmacokinetic model with a reduced number of fitting parameters, sacrificing biological specificity for improved accuracy.

The majority of clinical studies use a simple two-compartment pharmacokinetic model [27, 28] to estimates the transfer constant K^{trans} (bulk transfer coefficient, a quantity that depends on permeability and also blood flow) and v_e.

$$C_t(t) = K^{trans} \int_0^t C_p(t') \exp\left(\frac{-K^{trans}}{v_e}\right)(t-t')dt' \qquad (2)$$

where $C_t(t)$ is the concentration of agent in the voxel at time t and C_p is the concentration of agent in the plasma volume. This approach was designed for tissues with low vascular fractions and can give erroneously high values of K^{trans} in vascular tissues such as tumours. Consequently, it is more common to use an extension of this model (the modified Tofts model) which additionally enables calculation of the fractional plasma volume (v_p).

$$C_t(t) = v_p C_p(t) + K^{trans} \int_0^t C_p(t') \exp\left(\frac{-K^{trans}}{v_e}\right)(t-t')dt' \quad (3)$$

In these models, if the leak is small, then the rate at which gadolinium leaks out of capillaries is determined by permeability. Here, the blood flow is large enough to replace gadolinium that is lost through vessel leakage. The gadolinium concentration in the capillary is the same as in large arteries; there is no local depletion. Conversely, if the leak is large (large permeability surface area product, PS), then the rate at which gadolinium leaks out of capillaries may be limited by the blood flow (F; perfusion in ml of blood per min per ml of tissue) and not by PS. Formal mathematical analysis [29, 30] shows if PS<<F, then K^{trans}≈PS (permeability-limited), whereas if F<<PS, then K^{trans}≈F (flow-limited or perfusion-limited). For this reason, the quantity estimated termed K^{trans} does not relate simply to permeability or perfusion, although in very leaky tumours K^{trans} may in practice be perfusion limited.

K^{trans} has also been estimated from T_2 weighted DCE-MRI image data [31, 32]. This approach is less sensitive than T_1 weighted imaging, is relatively unreliable (since the relaxivity constant r_2* is unknown), and gives a limited number of slices. Its benefit is that it combines a DSC-MRI measurement of cerebral blood flow (CBF) with a leakage (permeability) measurement from a single bolus injection, and may prove to be a useful method of calculating vascular parameters while still accounting for vessel leakage.

The disadvantages of T_1 weighted DCE-MRI are mostly related to it being an immature technology. There remain considerable technical issues around measuring K^{trans} related to data collection and analysis techniques although the K^{trans} estimation technique outlined in this review is becoming a standard accepted approach and there is some degree of consensus on protocol standardisation [22, 33]. Measurement reproducibility is approximately 5–10% of the coefficient of variation [34, 35], similar to figures from competing techniques such as DSC-MRI, and this probably limits the sensitivity of the technique.

Endogenous contrast technique: arterial spin labelling

ASL is similar in essence to bolus tracking studies of perfusion: a ''tracer'' is introduced into the blood and the

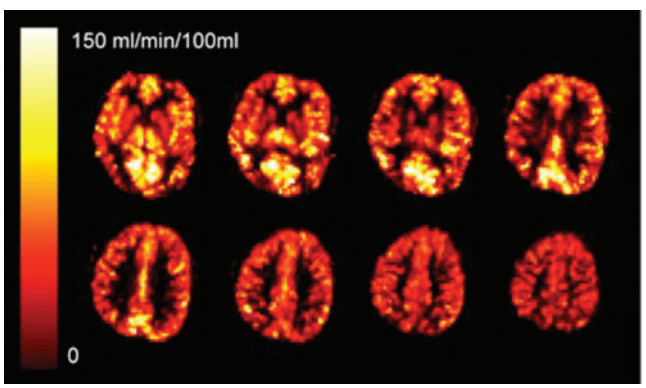

Figure 4. Quantitative maps of cerebral blood flow in the brain of a normal volunteer using a STAR PASL sequence at 3 T.

concentration of this tracer is tracked over time as it passes through the tissue of interest, which in practice is usually the brain. In the case of ASL, the tracer is endogenous water in the blood that is labelled magnetically using an radiofrequency (RF) inversion pulse. The technique can produce quantitative maps of perfusion, or cerebral blood flow, in units of $ml\,min^{-1}\,100\,ml^{-1}$.

Compared with dynamic contrast-enhanced approaches, the main advantage offered by ASL is its complete non-invasiveness, requiring no CA administration. This permits serial measurements, essential for certain applications such as fMRI. Another key advantage is the absolute quantification of perfusion offered by ASL. The main disadvantage is low SNR, requiring a number of averages to produce a good-quality image and taking approximately 10 min for whole-brain coverage. This improves at higher field strengths. ASL is not yet fully adopted by the manufacturers and hence local expertise may be needed for implementation.

The image acquisition technique involves collection of a pair of images: the label and the control image. The labelled image includes additional signal from labelled blood. On subtraction of the two images we obtain a perfusion-weighted image. The difference in signal between the two images is on the order of only 1%, so a number of averages are required. There are two principle labelling strategies.

(a) Continuous ASL (CASL): a spatially localised RF field positioned through the feeding arteries continuously inverts the longitudinal magnetisation of the protons in the blood as they flow through the plane [36]. The labelling pulse can cause large power deposition, which is a particular problem at higher field strengths. Owing to good coverage and high signal, CASL is particularly suited to resting state perfusion measurements.
(b) Pulsed ASL (PASL): a large volume of spins are labelled using a brief RF pulse. In the simplest technique [37] the labelling pulse is non-selective, whereas the control inversion covers only the slices of interest. Owing to the brief labelling pulse, acquisition of each image pair is faster than for CASL, making PASL particularly suited to functional imaging studies.

The main problems in image acquisition concern signal contributions that are unrelated to perfusion. First, the labelling pulse can cause additional signal in the tissue due to magnetisation transfer. This effect can be overcome either by using a separate labelling coil (CASL only) or by matching the magnetisation effects in the control image. Second, there is significant signal from background tissue. Application of a saturation pulse prior to labelling can reduce static tissue signal and improve SNR. Third, images may have substantial signal from large vessels. This can be overcome by applying diffusion gradients to dephase large vessel signal or by introducing a delay between labelling and signal collection to give time for fast-flowing blood in large vessels to flow into smaller vessels. Finally, some true perfusion signals may be missed if the transit time between the labelling plane and the imaging plane is long. A number of strategies to reduce the sensitivity to transit time effects have been developed [38, 39].

In order to produce accurate perfusion maps a number of factors need to be measured or assumed, including the degree of arterial spin inversion, the transit time from label to slice, the T_1 of blood and tissue, and the equilibrium magnetisation of arterial blood. Most applications use a single tissue compartment model [36], where the signal in the difference image $M(t)$, following labelling at time $t = 0$, can be described quite simply,

$$\frac{dM(t)}{dt} = -\frac{M(t)}{T_1} + f(m_a - m_v) \qquad (4)$$

where T_1 is the T_1 of tissue, f is perfusion, m_a is the arterial magnetisation and m_v the venous magnetisation. There is evidence that the labelled water remains largely intravascular at the time of imaging, and hence replacing T_1 with the T_1 of blood has been shown to be more accurate [40]. Further developments include corrections for transit time and restricted water diffusion [41].

A timely multicentre reproducibility study showed promising results [42], providing the reliability needed to proceed to clinical studies. A recent review paper [43] summarises major research areas, which include cerebrovascular disease, dementia, oncology and studies of normal brain function. One particular area of growth and interest is in the use of ASL for functional imaging, important for clinical studies where neurovascular coupling may be altered. ASL can be used in combination with blood oxygenation level-dependent (BOLD) imaging to quantify both blood flow and oxygenation changes [44], which could be of potential interest in tumour studies.

Conclusions

Advanced MRI and CT imaging techniques are becoming more widely available in conventional clinical practice. Although analysis and interpretation of the data derived from these techniques can be complex, many of the calculated parameters have physiological significance, are repeatable and have clear clinical uses in diagnosis, guiding therapy and in predicting patient outcome.

References

1. Jackson A, Buckley DL, Parker GJM. Dynamic Contrast-Enhanced Magnetic Resonance Imaging in Oncology 2005, Berlin, Germany: Springer.
2. Miles KA, Perfusion CT for the assessment of tumour vascularity: which protocol? Br J Radiol 2003;76:S36–42.
3. Miles KA, Griffiths MR. Perfusion CT: a worthwhile enhancement? Br J Radiol 2003;76:220–31.
4. Xie Q, Zhang J, Wu PH, Jiang XQ, Chen SL, Wang QL, et al. Bladder transitional cell carcinoma:correlation of contrast enhancement on computed tomography with histological grade and tumour angiogenesis. Clin Radiol 2005;60:215–23.
5. Wang JH, Min PQ, Wang PJ, Cheng WX, Zhang XH, Wang Y. Dynamic CT evaluation of tumor vascularity in renal cell carcinoma. AJR Am J Roentgenol 2006;186:1423–30.
6. Tateishi U, Kusumoto M, Nishhihara H, Nagashima K, Morikawa T, Moriyama N. Contrast-enhanced dynamic computed tomography for the evaluation of tumor angiogenesis in patients with lung carcinoma. Cancer 2002; 95:835–42.
7. Miles KA, Young H, Chica SL, Esser PD. Quantitative contrast-enhanced computed tomography:is there a need for system calibration? Eur Radiol 2007;17:919–26.

8. Gillard JH, Antoun NM, Burnet NG, Pickard JD. Reproducibility of quantitative CT perfusion imaging. Br J Radiol 2001;74:552–5.
9. Cenic A, Nabavi DG, Craen RA, Gelb AW, Lee TY. A CT method to measure hemodynamics in brain tumors: validation and application of cerebral blood flow maps. AJNR Am J Neuroradiol 2000;21:462–70.
10. Lee T-Y, Miles KA. Image processing. In: Miles KA, Cuenod C-A, editors. Multi-detector computed tomography in oncology: CT perfusion imaging. London, UK: Informa, 2007:61–72.
11. Youn SW,Kim JH, Wean YC, Kim SH, Han MK, Bae HJ. Perfusion CT of the brain using 40-mm-wide detector and toggling table technique for initial imaging of acute stroke. AJR Am J Roentgenol 2008;191:W120–6.
12. O'Connor JPB, Jackson A, Asselin MC, Buckley DL, Parker GJM, Jayson GC. Quantitative imaging biomarkers in the clinical development of targeted therapeutics current and future perspectives. Lancet Oncol 2008;9:756–66.
13. Miles KA. Perfusion CT-PET: opportunities for combined assessment of tumor vascularity and metabolism. In: Miles KA, editor. Multi-detector computed tomography in oncology: CT perfusion imaging. London, UK: Informa, 2007.
14. Calamante F, Thomas DL, Pell GS, Wiersma J, Turner R. Measuring cerebral blood flow using magnetic resonance imaging techniques. J Cereb Blood Flow Metab 1999;19:701–35.
15. Li KL, Zhu XP, Jackson A. Parametric mapping of scaled fitting error in dynamic susceptibility contrast enhanced MR perfusion imaging. Br J Radiol 2000;73:470–81.
16. van Gelderen P, Grandin C, Petrella JR, Moonen CTW. Rapid three-dimensional MR imaging method for tracking a bolus of contrast agent through the brain. Radiology 2000;216:603–8.
17. Jackson A, O'Connor J, Thompson G, Mills S. Magnetic resonance perfusion imaging in neuro-oncology. Cancer Imaging 2008;8:186–99.
18. Batchelor TT, Duda DG, di Tomaso E, Ancukiewicz M, Plotkin SR, Gerstner E, et al. Phase II study of cediranib, an oral pan-vascular endothelial growth factor receptor tyrosine kinase inhibitor, in patients with recurrent glioblastoma. J Clin Oncol 2010;28:2817–23.
19. Jackson A, Kassner A, Annesiey-Williams D, Reid H, Zhu XP, Li KL. Abnormalities in the recirculation phase of contrast agent bolus passage in cerebral gliomas:comparison with relative blood volume and tumor grade. AJNR Am J Neuroradiol 2002;23:7–14.
20. Ostergaard L, Johannsen P, Høst-Poulsen P, Vestergaard-Poulsen P, Asboe H, Gee AD, et al. Cerebral blood flow measurements by magnetic resonance imaging bolus tracking:comparison with [(15)O]H_2O positron emission tomography in humans. J Cereb Blood Flow Metab 1998;18:935–40.
21. Parker GJ, Roberts C, Macdonald A, Buonaccorsi GA, Cheung S, Buckley DL, et al. Experimentally-derived functional form for a population-averaged high-temporal-resolution arterial input function for dynamic contrast-enhanced MRI. Magn Reson Med 2006;56:993–1000.
22. Leach MO, Brindle KM, Evelhoch JL, Griffiths JR, Horsman MR, Jackson A, et al. The assessment of antiangiogenic and antivascular therapies in early-stage clinical trials using magnetic resonance imaging:issues and recommendations. Br J Cancer 2005;92:1599–610.
23. Evelhoch JL. Key factors in the acquisition of contrast kinetic data for oncology. J Magn Reson Imaging 1999;10:254–9.
24. St Lawrence KS, Lee TY. An adiabatic approximation to the tissue homogeneity model for water exchange in the brain: I. Theoretical derivation. J Cereb Blood Flow Metab 1998; 18:1365–77.
25. Jackson A, O'Connor JP, Parker GJ, Jayson GC. Imaging tumor vascular heterogeneity and angiogenesis using DCE-MRI. Clin Cancer Res 2007;13:3449–59.
26. Buckley DL, Kerslake RM, Blackband SJ, Horsman A. Quantitative analysis of multi-slice Gd-DTPA enhanced dynamic MR images using an automated simplex minimization procedure. Magn Reson Med 1994;32:646–51.
27. Tofts PS. Modeling tracer kinetics in dynamic Gd-DTPA MR imaging. J Magn Reson Imaging 1997;7:91–101.
28. Tofts PS. Measurement of the blood-brain barrier permeability and leakage space using dynamic MR imaging. 1. Fundamental concepts. Magn Reson Med 1991;17: 357–67.
29. Barrett T, Brechbiel M, Bernardo M, Choyke PL. MRI of tumor angiogenesis. J Magn Reson Imaging 2007;26:235–49.
30. Tofts PS, Brix G, Buckley DL, Evelhoch JL, Henderson E, Knopp MV, et al. Estimating kinetic parameters from dynamic contrast-enhanced T(1)-weighted MRI of a diffusable tracer:standardized quantities and symbols. J Magn Reson Imaging 1999;10:223–32.
31. Law M, Kazmi K, Wetzel S, Wang E, Lacab C, Zagzag D, et al. Dynamic susceptibility contrast-enhanced perfusion and conventional MR imaging findings for adult patients with cerebral primitive neuroectodermal tumors. AJNR Am J Neuroradiol 2004;25:997–1005.
32. Provenzale JM, Wang GR, Brenner T, Petrella JR, Sorensen AG. Comparison of permeability in high-grade and low-grade brain tumors using dynamic susceptibility contrast MR imaging. AJR Am J Roentgenol 2002;178:711–16.
33. O'Connor JP, Jackson A, Parker GJM, Jayson GC. DCE-MRI biomarkers in the clinical evaluation of antiangiogenic and vascular disrupting agents. Br J Cancer 2007;96:189–95.
34. O'Connor JPB, Carano RAD, Clamp AR, Ross J, Ho CCK, Jackson A, et al. Quantifying antivascular effects of monoclonal antibodies to vascular endothelial growth factor: insights from imaging. Clin Cancer Res 2009;15:6674–82.
35. Galbraith SM, Lodge MA, Taylor NJ, Rustin GJ, Bentzen S, Stirling JJ, et al. Reproducibility of dynamic contrast-enhanced MRI in human muscle and tumours: comparison of quantitative and semi-quantitative analysis. NMR Biomed 2002;15:132–42.
36. Detre JA, Leigh JS, Williams DS, Koretsky AP. Perfusion imaging. Magn Reson Med 1992;23:37–45.
37. Kim HS, Kim SY, Kim JM. Underestimation of cerebral perfusion on flow-sensitive alternating inversion recovery image: semiquantitative evaluation with time-to-peak values. AJNR Am J Neuroradiol 2007;28:2008–13.
38. Luh WM, Wong EC, Bandettini PA, Hyde JS. QUIPSS II with thin-slice TI1 periodic saturation:a method for improving accuracy of quantitative perfusion imaging using pulsed arterial spin labeling. Magn Reson Med 1999;41:1246–54.
39. Alsop DC, Detre JA. Reduced transit-time sensitivity in noninvasive magnetic resonance imaging of human cerebral blood flow. J Cereb Blood Flow Metab 1996;16:1236–49.
40. Parkes LM, Tofts PS. Improved accuracy of human cerebral blood perfusion measurements using arterial spin labeling: accounting for capillary water permeability. Magn Reson Med 2002;48:27–41.
41. Parkes LM. Quantification of cerebral perfusion using arterial spin labeling: two-compartment models. J Magn Reson Imaging 2005;22:732–6.
42. Petersen ET, Mouridsen K, Golay X. The QUASAR reproducibility study, Part II:Results from a multi-center Arterial Spin Labeling test-retest study. Neuroimage 2010;49:104–13.
43. Brown GG, Clark C, Liu TT. Measurement of cerebral perfusion with arterial spin labeling: Part 2. Applications. J Int Neuropsychol Soc 2007;13:526–38.
44. Buxton RB, Uludağ K, Dubowitz DJ, Liu TT. Modeling the hemodynamic response to brain activation. Neuroimage 2004;23:S220–33.